"Sapienza" Università di Roma

Facoltà di Medicina ed Odontoiatria

Dottorato di Ricerca

in

"Tecnologie Innovative nelle Malattie dello Scheletro,
della Cute e del Distretto Oro-Cranio-Facciale"
Ciclo XXX

Coordinatore
Chiar.ma Prof.ssa Antonella Polimeni

In Vitro Assessment of Normal and Pathological Dental Structures by Nuclear Magnetic Resonance Micro-Imaging at High Field

Tutor
Chiar.mo Prof. Luca Testarelli

Candidato
Dott. Dario Di Nardo
Matricola 1048490

ABSTRACT

Aims: Aim of this work is to analyze the various field of application of Magnetic Resonance Imaging in endodontics and highlight its current advantages and limitations due to understand its future application in research and clinical practice. The effectiveness in revealing the presence or absence of a pathological condition affecting enamel, dentin, endodontic space and the quality of the apical seal of an endodontic sealing technique was investigated.

Materials and methods:

Three extracted monoradicular teeth were analyzed using a Bruker Avance-400 high-resolution spectrometer operating at 9.4 T with a micro-imaging probe (10 mm internal diameter), equipped with a gradient unit characterized by a maximum gradient strength of 1200 mT/m and a rise time of 100 μs.

XWINNMR® and ParaVision® 3.0 software were employed for data acquisition and analysis.

Images of teeth were weighted in T_2 at different TE to measure T_2 relaxation times and in Apparent Diffusion Coefficient (ADC) in different regions of interest (ROI).

Results: T_2 and ADC values were obtained at different ROI. Clear images of carious lesions, periodontal tissues, pulpar remnants and endodontic materials such as guttapercha cones were acquired. Presence of microcracks and a calcification of the pulp were also clearly differentiated.

Conclusions: Micro MRI is a non-invasive, non-destructive tool for the assessment of pathological conditions affecting dental hard and soft tissues, and it may help in finding endodontic procedural mistreatments such as incomplete detersion or inadeguate tridimensional filling *in vitro*.

INDEX

1. INTRODUCTION

Three-dimensional (3D) images of the human body in mandibular, maxillar and temporal areas of the human head, are currently acquired by computed tomography (CT), conebeam computed tomography (CBCT) and by magnetic resonance imaging (MRI) devices. MRI has become fundamental for non-invasive diagnosis of soft tissue diseases without using ionizing radiations. It is almost comparable with CBCT in terms of spatial resolution and offers the possibility to visualize data in cross sectional and panoramic view, more familiar to dentists. [1]

MRI is based on Nuclear Magnetic Resonance (NMR) spectroscopy that is performed by stimulating with an electromagnetic field in the range of radiofrequencies (RF), spins of hydrogen nucleus immersed in a strong magnetic field B_0 which is able to magnetize and line up the majority of them. Signals from no more excited spins returning to the initial position, are received by a radiofrequency probe as induced electromotive force to the hands of the same probe. The acquired signal decays exponentially in time due to spin-spin and spin-lattice relaxation processes, which are quantified by the T_2 and T_1 parameters, respectively. Moreover, the signal is characterized by an own frequency response that provides physical-chemical information about the investigated tissues.

Superimposing to the main magnetic field, controlled magnetic field gradients along x, y and z axis, images are obtained similarly to

computerized tomography scanners [2, 3].

Manipulating the duration and the shape of the radiofrequency pulses that excites the nuclear spins, or the direction and strength of the field gradients, a specific plane or volume of interest can be selected in different orientations. A 3D MRI scanning is composed by several 2D images of a selected thickness. NMR signals are processed by a computer that re-constructs the MRI images (essentially a map of the spatial distribution of hydrogen nuclei) using algorithms based on the Fourier transform [4, 5].

MRI in dentistry is currently performed most for diagnosing temporo-mandibular joint disorders and to evaluate extension of tumours and osteomyelitis [6]. Since MRI does not use ionizing radiation, it is particularly relevant for repeated examinations in children [4, 7].

Aim of this work is to analyze the various field of application of MRI in endodontics and highlight its current advantages and limitations due to understand its future application in research and clinical practice. The effectiveness in revealing the presence or absence of a pathological condition affecting enamel, dentin, endodontic and periodontal system, was examined using a high field (9.4 Tesla) magnetic resonance device for experimental applications: the quality of the apical seal of an endodontic technique was even investigated.

1.1 Dental RMI

MRI has been proposed for diagnosis, treatment planning and evaluation of the outcome in endodontics: imaging the internal anatomy of the tooth can be quite difficult due to small volumes of these structures. The pulp chamber volume of a tooth can range from 0.006 mm^3 for the lower incisor to 0.068 mm^3 for the upper molar. Furthermore, the endodontic system can be very complex. Film-based or digital conventional radiographic techniques have several limitations, such as the two-dimensional nature of the produced images, anatomical noise or geometric distortion [8].

It has been known since the discovery of NMR that various spins in a heterogeneous sample can be classified by their spin-spin relaxation times (T_2). The sizes of the spin groups can be determined if the total free induction decay (FID) of the sample can be resolved into magnetization "components" decaying with the different T_2. [9]

In 1984, Funduk *et al.,* measured T_2 relaxation time and magnetization of protons in the human enamel, exploiting solid-like interstitial water (T_2~14 microseconds), enamel apatite (T_2~61 microseconds) and semiliquid-like water components (T_2~240 microseconds). These relaxation times are quite short to be observed in conventional MRI and bounded water component in the enamel was evaluated only ~1-2% in weight [10].

Dentin contains ~35% of organic matter and water and 65% is inorganic material, mainly hydroxyapatite. The natural blotted dentin contains protons in water (50%), proteins (45%) and apatite (5%); 52% of the water is associated with the surfaces of hydroxyapatite and with the collagene and protein matrix of the dentin, similarly to the water hydrating a large molecule. At least, the 18% of the water is trapped in the dentinal tubules. Differently from enamel, dentin T_2 is longer, but only ~10% of the magnetization exceed 250 microseconds [9].

Conventional MRI requires signals characterized by spin-spin relaxation time higher than 2 milliseconds. As consequence, the mineralized tissues such as dentin and enamel, will result in a black zone due to the impossibility of capturing their signals by the device. Conversely, pulp and periodontal tissues, which are soft tissues and therefore more hydrated, will be acquired properly and appear white or gray in the NMR image [11].

In vitro studies can reach better performance in terms of resolution due to the longer acquisition time (minutes to hours) and the stronger magnetic field used (7.04 - 9.4 Tesla): *in vivo* imaging is usually performed with lower fields (typically 1.5 or 3 Tesla) and the resolution depends highly on gradient strengths, coil configuration, patient comfort, and motion control [11, 12].

While hard tissue can be more easily visualized by traditional

radiology, MRI is easier to investigate soft dental tissue. In fact, as opposed to hard dental tissues, soft dental tissues have higher water content and much longer T_2 relaxation times. Based on these concepts, it was proposed that a high MRI signal of soft dental tissues could enable a high-resolution imaging of a dental pulp anatomy. An initial attempt in this direction was done by Lockhart *et al*. (1992), who utilized a strong 9.4 T magnetic field to obtain MR images of the pulp chamber *in vitro* and to visualize the tooth outline [13, 14]. Sustercic and Sersa (2012) demonstrated that MR microscopy could provide very accurate 3D visualization of dental pulp anatomy *in vitro*. MRI can detect signal of soft tissues as the dental pulp, that cannot be directly acquired by radiographic imaging. Conventional x-rays can directly fine detect only hard dental tissues, whereas the pulp anatomy can be estimated only by interpreting signal voids between hard dental tissues. The strong MRI signal from these soft tissues can be used for the assessment of the dental pulp anatomy, either in a sequence of 2D slices or by volume rendered projections of the pulp. [15]

1.2 Signal to noise ratio and image resolution in MRI

The nucleus of a hydrogen atom, has a nuclear moment that can be described as a small magnet. In a stable, non-interactive state, the magnet will be randomly oriented. If we apply a magnetic field to the atom, it will be no longer oriented randomly, but it will re-orientate itself parallel or antiparallel to the magnetic field, depending on the energy imparted to the nuclear magnetic moment.

With the application of a magnetic field, the original single energy level of the hydrogen atom will be split into two Zeeman levels (+1/2 or lower level and -1/2 or higher level). In NMR, transitions (or resonances) between Zeeman levels are induced by applying radiowaves that match exactly the energy differences between the levels. Once atoms are transformed in the excited state by the application of radiowaves, the nuclear magnetic moment will decay exponentially by relaxation processes to the ground state and meanwhile atoms will emit radiowaves that can be received by the RF probe and then amplified for improving the signal-to-noise ratio (SNR).

Radiowaves emitted by the excited atoms depend on both the density of the excited atoms and the time required for the atoms to return to the ground state; these properties may be used to optimize signal, suppressing background noise [4].

The SNR is measured by calculating the ratio between the signal

intensity in an area of interest and the standard deviation (SD) of the signal from the background (in an area chosen out from the object).

The image resolution is quantified by the image voxel size. More specifically, the base area of the voxel provides the in-plane resolution of the image, while the height of the voxel is determined by the slice thickness of each bi-dimensional image. Image resolution strongly depends on magnetic gradients strength of imaging gradients. In clinical scanners, the maximum gradient strength is around 40mT/m and 80mT/m depending on NMR companies and on scanner model.

SNR is proportional to the volume of the voxel and to the square root of the number of averages (NA). Since averaging takes time, SNR is related closely to the acquisition time.

In MRI, the SNR can be improved by increasing voxel size, reducing the bandwidth using surface coils, using an echo time (TE) of spin echo sequence as short as possible and increasing the number of signal acquisitions (NA). Voxel size can be increased by increasing the field of view (FOV), decreasing the matrix size, increasing the slice thickness (STK).

All the actions that increase SNR, decrease the image resolution: new strategies should be used to perform dental MRI with a good compromise between SNR and image resolution [1, 4-6].

1.3 RF and imaging gradient coils

A good strategy to reduce FOV for increasing the image resolution without lowering the SNR is to use dedicated RF coils.

Head or neck coils cannot reach the resolution needed for practical dental applications: extra-oral placement of the coil can results in images that will contain more signals from less important tissues as the fat of the cheek. In other words, head-neck RF coils provide a large FOV that, together with the limited imaging gradient strength of clinical scanners, can provide image with a maximum in plane resolution of 300x300 μm^2.

Intraoral positioning of the RF coil may increase both resolution and SNR but it can be difficult to implement it due to anatomical differences as the presence of tori and frenula that will avoid the most distal elements or apical thirds of the teeth to appear in the acquired volume. One of the most comfortable coil position was proposed by Idiyatullin *et al.* (2014), who explained the advantages of using a loop coil in the occlusal position for dental applications, the coil's shape is similar to an impression tray and it can be kept in the mouth between dental arches [16]. The high patient comfort and the increased signal sensitivity of a dedicated coil may be helpful for implementing future imaging sequences which need very high excitation and receiving bandwidths [17].

Ludwig U *et al. (*2016) from a 3D-FLASH MRI sequence, obtained a volume of 64·64·28 mm^3 with a voxel size of ~250-250-500 μm^3

(resolution ~350 μm^3) in 3:57 minutes *in vivo* using a wireless intraoral coil at 3 T) with a quality image comparable to CBCT. Gingiva, pulp, cancellous bone, inferior alveolar nerve with branches and the periodontium were represented in detail [18].

1.4 Artifacts

A study on the affection of dental materials on NMR signal [19], showed that composites, amalgam, gold and Ni-Ti alloys can produce relatively strong artifacts; stainless steel brackets or wires can produce voids in the signal. These materials may alter the precession frequencies of hydrogen nucleus spins and distort the linear magnetic field gradients, resulting in signal loss from spin dephasing and mismapping artifacts associated with frequency shifts. In the case of high-resolution dental MRI applications, such as diagnosis of caries or MRI-based dental impressions, it is strongly recommended to use compatible composite materials in the tooth of interest and in the adjacent areas as neighbors teeth or antagonists. Even a small distortion caused by the presence of a non compatible material, as a cavity in the tooth or post in the dental root can make the results of the measurements useless.

Glass ionomer cement, gutta-percha, zirconium dioxide and some composites resulted to be fully compatible with the MRI as they can be present even in the tooth of interest. Polycarboxylate and zinc phosphate based cement, some modified dimethacrylates can produce small image artifacts [20, 21].

1.5 Technical Issues

The NMR signal decays over time due to the spin-spin relaxation, quantified by the parameter T_2, indicating how quickly the signal is canceled (goes to zero) and spin-lattice relaxation, quantified by the time constant T_1, indicating how quickly the system returns to the initial equilibrium state (the one it had before absorbing radio frequency).

Conventional MRI performed in clinical scanners are characterized by hardware and software to acquire signals with T_2 higher than 2 ms. As T_2 relaxation time of human enamel runs from about 14 to 61 μs and in mineralized dentine, only ~10% of the NMR signal exceed 250 μs; [9, 10] the mineralized tissues in dentin and enamel, will be not acquired properly, instead of soft tissues and pulp which could be fine represented [22, 23].

In vitro studies can reach better performance in terms of resolution due to the higher SNR provided by high magnetic field (higher than 7 T), higher magnetic field gradient (higher than 300 mT/m), reduced FOV, the possibility of carrying out many of the signal average (NA) [22] and the possibility of using MRI acquiring sequences with very short echo times (TE) [24].

2. MATERIALS AND METHODS

Three extracted monoradicular teeth were analyzed using micro-MRI technique to investigate pathological conditions affecting hard and soft tissues *in vitro*. Teeth were kept in a NaCl 0,9% solution for two days at 4°C before the acquisitions and then inserted in a 1 cm diameter glass capillar for magnetic resonance (Kontes Glass Company, Vineland, New Jersey, USA). The capillary was filled with distilled water and the sample temperature was fixed to 25 °C.

MRI experiments were performed at the NMR laboratory of CNR ISC, Physics Department of "Sapienza" University of Rome, using a Bruker Avance-400 high-resolution spectrometer operating at 9.4 T with a micro-imaging probe (10 mm internal diameter), equipped with a gradient unit characterized by a maximum gradient strength of 1200 mT/m and a rise time of 100 μs. XWINNMR® and ParaVision® 3.0 software were employed for data acquisition and analysis.

NMR acquired images were exported in DICOM format to a post-processing workstation (Z800 HP, California, USA). Fitting procedures in each voxel and image post processing were performed to obtain T_1, T_2 and ADC maps. T_1, T_2 and ADC values were calculated in region of interest (ROI) indentified in NMR maps.

The first specimen was an extracted upper canine, which crown was opened with a spherical diamond bur and partially treated using an

endodontic k-file #10 and immersed in distilled water.

Image was weighted in T_2 at different TE, to measure T_2 in different Region of Interest (ROI), called ISA, using the following acquisition parameters: multi-slice multi echo MSME sequence, TR=4000 ms, NS=32, TE da 2.8 ms a 44 ms in 15 different ROI (Figure 1). Pulpar tissues from the first specimen were also weighted in Apparent Diffusion Coefficient ADC with b-value = 640 and 1440 mm^2/s (Figure 2).

Second specimen, an inferior supernumerary central incisor, which was subjected to excessive occlusal forces that irreversibly damaged the buccal cortical bone, was extracted due to mobility and pain.

Images of the second specimen were obtained by using a 9.4 T magnetic field, a multi-slice multi echo MSME sequence with echo time TE=3 ms, repetition time TR=5000 ms, slice thickness of each image slice STK=0.5mm, in plane resolution 62x62 μm^2 (Figure 3 and 4).

A multi-slice multi echo sequence MSME, T_2w: repetition time, TR=4500ms; field of view, FOV=10x10mm2; image matrix 256x256; slice thickness, STH=0.3mm; voxel dimension 39x39μm^2, number of averaged scans NS=64, number of slices=48 (Figure 5).

A multi-slice multi echo sequence MSME with echo time TE=2.2ms, repetition time TR=1800ms, slice thickness of each image slice STK=0.2mm, in plane resolution 58x58 μm^2 (figure 6).

For the acquisition of the third specimen (Figure 7), an endodontic

treated radicular remnant, two MSME (Multi Slice Multi Echo) imaging sequences with the following parameters were used: repetition time, TR=2000ms; field of view, FOV=15x15mm^2; image matrix 256x256; slice thickness, STH=0.3mm; voxel dimension 58x58μm^2, number of averaged scans NS=32; were performed at various TEs (24 TEs from 2.3ms to 55.2ms), for obtaining spin echo (SE) decay from which to extract T_2 values in each image voxel (T_2-map) in two different view: coronal and axial. Moreover, to obtain coronal and axial T_1-maps, two MSME imaging sequence with the following parameters: TE=1.8 ms, FOV=15x15mm^2, image matrix 256x256, STH=0.3mm, voxel dimension 58x58x300μm^3, NS=32, were performed at TR= 2000ms, 900mas, 500ms, 300ms. Finally, an axial Pulse gradient Stimulated echo (PGSTE) imaging sequence was also employed (TE/TR=11.3/2500ms, FOV=7mm, matrix 128x128, diffusion time Δ=60ms, diffusion gradient duration δ=3ms, using three effective b-values: 167, 1467 and 3167 s/mm^2, diffusion gradient direction along the x direction, STH=0.6mm, NS=64) in order to obtain the apparent diffusion coefficient (ADC)-map with voxel dimension 58x58x600μm^3. The b value, that select the molecular diffusion regime, is related to the aforementioned parameters through the known relation: $b=\gamma^2 g^2(\Delta-\delta/3)$, where g is the diffusion gradient strength, δ is the gradient pulses duration and Δ is the temporal interval during which the diffusion processes are observed.

Cone Beam Computed Tomography of all the samples were performed to evaluate differences between radiological examination and RMI: acquisitions were performed with a CBCT (KaVo Gendex CB500) with the following volumetric acquisition protocol: 5 mA, 120 kV, slice thickness 0,125 mm, FOV 8,9x3,0 cm, voxel dimension 0,125x0,125×0,125 mm. Images were processed by a desktop pc equipped with iCATVision™ (Imaging Sciences International, Hatfield, Pennsylvania).

3. RESULTS

In the present study MRI was used to detect caries, microcracks, quality of canal obturation and the presence of pulpar remnants into the endodontic space. In detail, MRI has exploited the ability of water to fill all tooth spaces to highlight endodontic canals, decays, periodontal remains, lateral canals, microcracks and to evaluate the effectiveness of an endodontic treatment.

By the analysis of the first specimen, different T_2 values were extracted at different ROI: distilled water with paramagnetical impurities originating from the tooth, $T_2 = 600\pm200$ ms; hydrated soft tissues, $T_2 = 63\pm6$ ms; more structured hydrated tissues such as vessels or lymphatic remnants, $T_2 = 28\pm3$ ms; nerves, $T_2 = 15,3\pm0,8$ ms (Figure 1).

Weighting the first specimen with Apparent Diffusion Coefficient, following values were obtained (Figure 2): distilled water, ADC = $2*10^{-3}$ mm^2/s; free soft tissues, ADC = $1*10^{-3}$ mm^2/s; more structured soft tissues as vessels and lymphatic ducts, ADC = $0.6*10^{-3}$ mm^2/s; nerves, ADC = $0.88*10^{-3}$ mm^2/s.

For the second specimen, MRI showed well defined images of the border of the demineralized tissue and it was clearly recognizable the shape of the endodontic canal and periodontal remains (Figure 3). Small structures such as lateral canal in the apical third could be recognizable (Figure 4): it can be differentiate from a microcrack because it's visible

only in few images, despite of a microcrack which can be present in all the images representing the area of interest (Figure 5).

The resolution of the MRI device also shown the presence of microcrack affecting the coronal third and projecting to the endodontic space, in addition it can be visible a pulpar calcification sorrounded by hydrated tissues (Figure 6).

Evaluating the effectiveness of and endodontic treatment, we appreciate the presence of two guttapercha cones sorrounded by a well hydrated area: an incomplete three-dimensional filling that allowed infiltration of water from the apical foramen, which is situated on the interproximal surface before the anatomical apex, could be fine recognized (Figure 7).

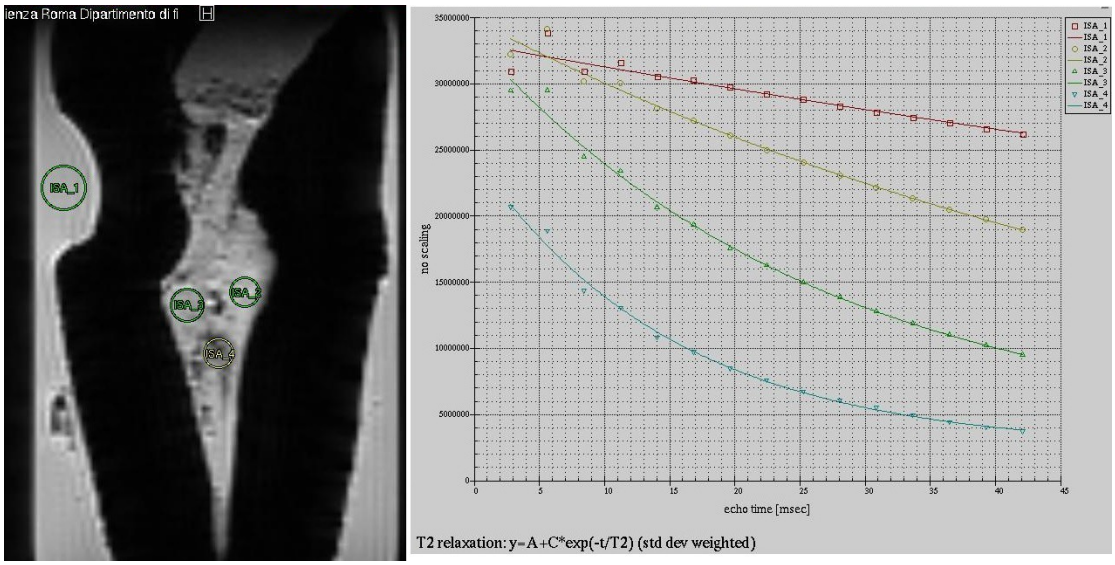

Figure 1. Image of the first specimen weighted at T_2 with different TE. Acquisition parameters: MSME, TR=4000 ms, NS=32, TE from 2.8 ms to 44 ms at 15 different ROIs (ISA). The graph shows the relaxation times value at different echo times: distilled water, T_2 = 600±200 ms; hydrated soft tissues, T_2 = 63±6 ms; more structured hydrated tissues such as vessels or lymphatic remnants, T_2 = 28±3 ms; nerves, T_2 = 15,3±0,8 ms. Fit function used to extract T_2 is reported at the end of the graph.

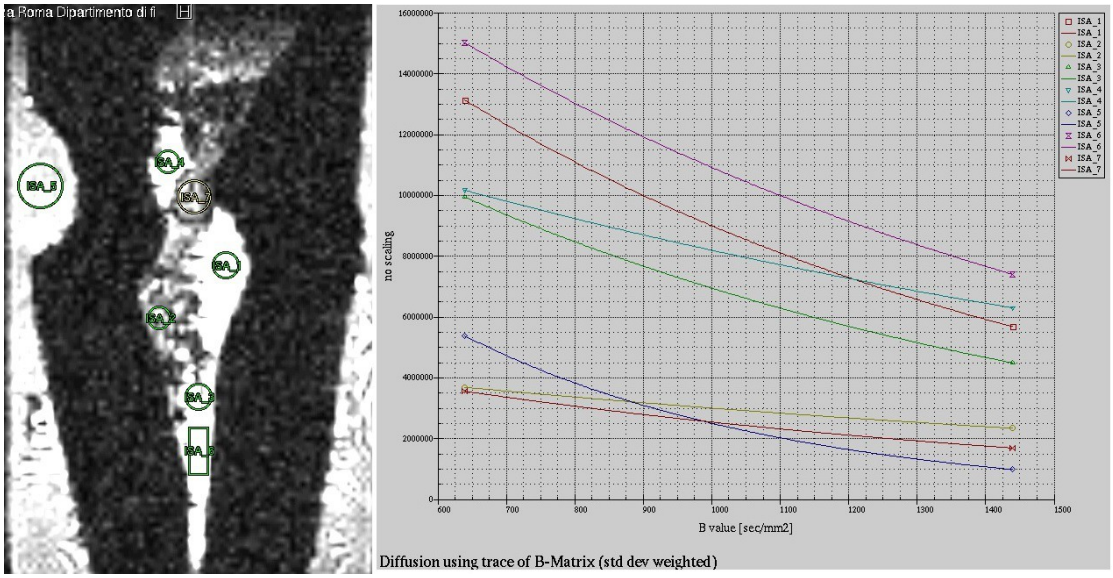

Figure 2. Image of the first specimen weighted in Apparent Diffusion Coefficient (ADC), b-value = 640 and 1440 mm^2/s. Diffusion values at different b-values are reported in the graph: distilled water, ADC = $2*10^{-3}$ mm^2/s (ISA 5); free soft tissues, ADC = $1*10^{-3}$ mm^2/s (ISA 1 and 3); more structured soft tissues as vessels and lymphatic ducts, ADC = $0.6*10^{-3}$ mm^2/s (ISA 2 and 4); nerves, ADC = $0.88*10^{-3}$ mm^2/s (ISA 7).

Figure 3 – Carious lesion affecting the interproximal surface. The tooth was immersed into a NMR glass tube filled of water of 8 mm in diameter. It can be visible the border of the demineralized tissue. It's clearly recognizable the shape of the endodontic canal and periodontal remains. The image was obtained by using a 9.4 T magnetic field, a multi-slice multi echo sequence with echo time TE=3 ms, repetition time TR=5000 ms, slice thickness of each image slice STK=0.5 mm, in plane resolution 62x62 μm^2.

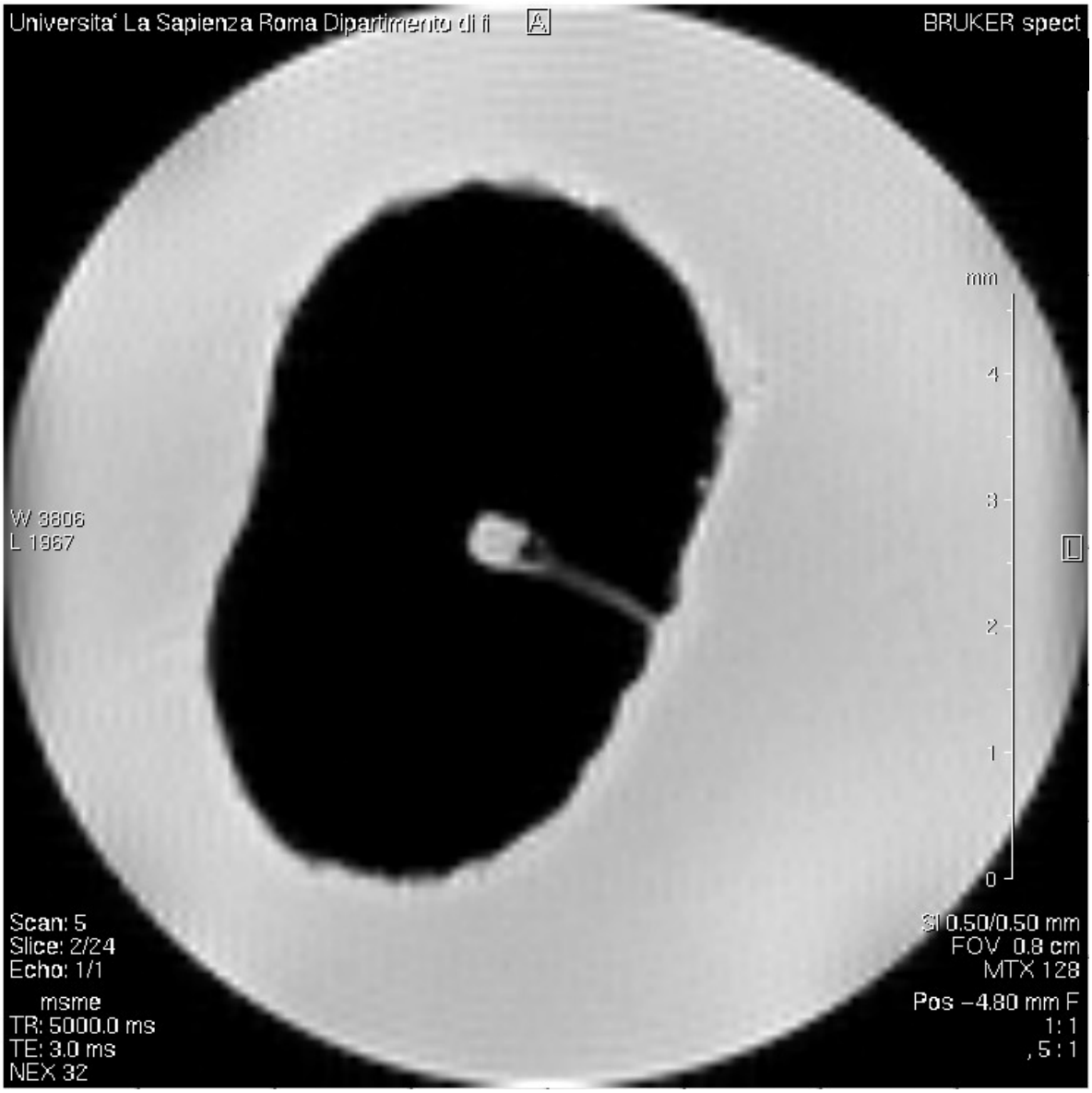

Figure 4 – A lateral canal in the apical third. It can be differentiate from a microcrack because it's visible only in few images, despite of a microcrack which can be present in all the images representing the area of interest. The image was obtained by using a 9.4 T magnetic field, a multi-slice multi echo sequence with echo time TE=3 ms, repetition time TR=5000 ms, slice thickness of each image slice STK=0.5 mm, in plane resolution 62x62 μm^2.

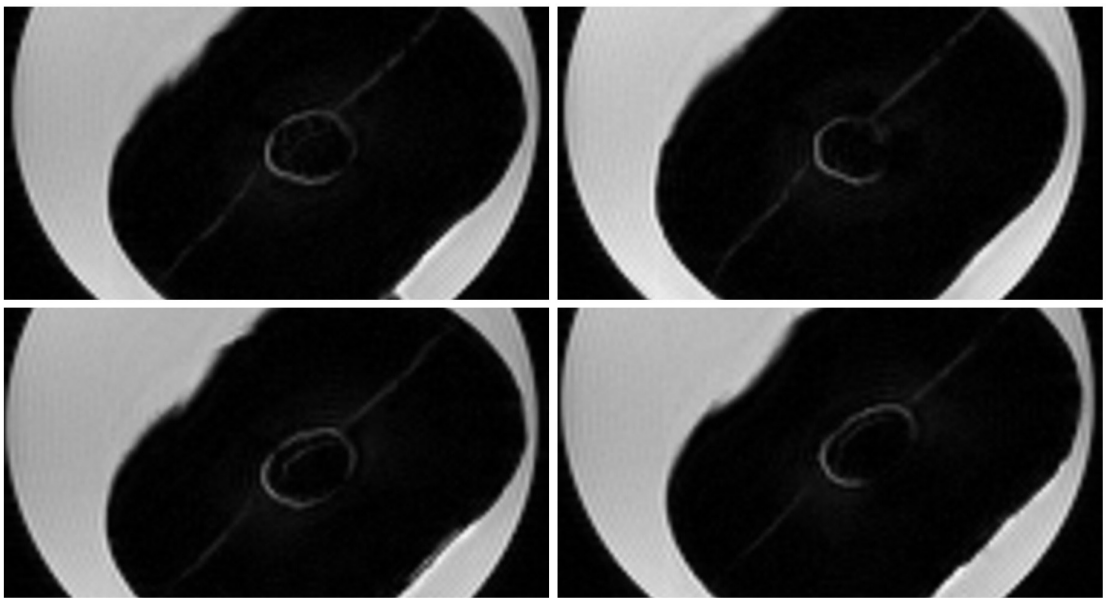

Figure 5 - Vertical microcracks affecting both interproximal surfaces of the tooth are evidenced by the infiltration of water at various sections of the sample. The image was obtained by using a 9.4 T magnetic field, MSME were employed to obtain axial view. T2w: repetition time, TR=4500 ms; field of view, FOV=10x10 mm2; image matrix 256x256; slice thickness, STH=0.3 mm; voxel dimension 39x39 μm2, number of averaged scans NS=64, number of slices=48.

Figure 6 – A microcrack affecting the coronal third projecting to the endodontic space and a pulpar calcification sorrounded by hydrated tissues. The tooth was immersed into a NMR glass tube filled of water of 8 mm in diameter. The image was obtained by using a 9.4 T magnetic field, a multi-slice multi echo sequence with echo time TE=2.2 ms, repetition time TR=1800 ms, slice thickness of each image slice STK=0.2 mm, in plane resolution 58x58 μm^2.

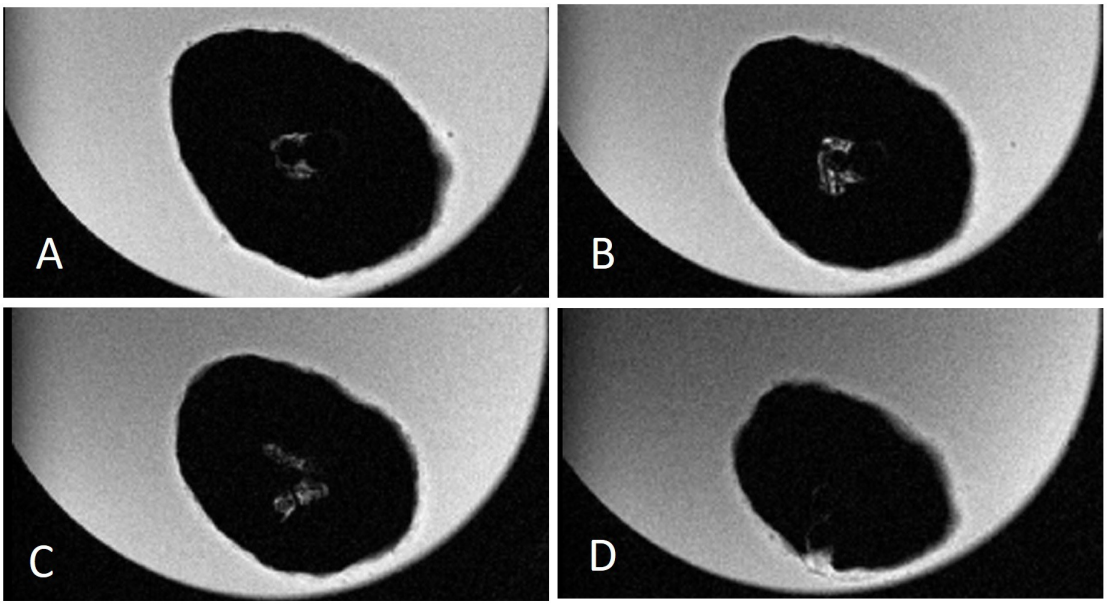

Figure 7 – In the sequence of axial view images of a tooth endodontically treated and immersed into a NMR tube filled of water, the presence of two guttapercha cones sorrounded by a well hydrated area is recognizable (A and B). An incomplete three-dimensional filling allowed infiltration of water from the apical foramen (C), which is situated on the interproximal surface before the anatomical apex (D).

MSME sequence was used with the following acquisition parameters: TE=2.4 ms, TR=1500 ms, STK=0.4 mm, in plane resolution 35x35 μm^2.

4. DISCUSSION

Magnetic resonance imaging is nowadays a well-established imaging modality that is used in various medical fields as well as in material's science. Among medical MRI applications it is also an emerging field in dentistry which include detection of early bone changes such as neoplasm, fractures, inflammatory conditions, as well as imaging of mouth floor, tongue, salivary glands and TMJ. MRI in dental applications can be divided into imaging of soft dental tissues (dental pulp and periodontal tissues) and hard dental tissues (enamel and dentin).

Microscopic MRI seems to be well suited to studying the development of dental caries: it is non-destructive and non-invasive, does not use ionizing radiations and leaves tissues available for further investigations [23].

To visualize mineralized tissues of the teeth some authors proposed techniques based on short TE time acquisition, as stray field imaging (STRAFI), single and multinuclear solid state techniques, single-point imaging (SPI), sweep imaging with Fourier transformation (SWIFT), zero echo time imaging (ZTE) and Ultrashort Echo time (UTE) imaging and Free Induction with Steady State Procession (FISP), but actually, none of these techniques can produce satisfying diagnostic images of calcified tissues within reasonable scanning times [25, 26, 27].

In this study, multi-slice multi echo MSME and ADC sequences have

been used to visualize microscopical aspects of extracted teeth *in vitro*. Acquisitions were performed to obtain many informations as possible so it aimed to reach the highest resolution available for the device: this objective has prolonged acquisition times for each sample to ~20 hours. Images of hard structures and endodontic space were fine detailed and it was possible to appreciate the presence of decay, pulpar remnants, lateral canals, microcracks and endodontic fillings with incomplete three-dimensional sealing.

Measurements of the T_2 and ADC mapping showed the presence of interstitial water, soft tissue remnants, debris and nerves in partially treated endodontic space. These measurements let the clinician to differentiate the nature of the various tissues and compounds and exactly localize them in space (Figures 1 and 2).

Because of its ~40% in volume of water content, dental hard tissues are not able to be acquired properly with clinically used magnetic resonance devices. Conventional MR sequences are not designed to detect the fast decaying signal of teeth, but pulp, periodontal soft tissues and oral fluids could be more easily acquired. The MSME sequences used in this study was not capable to differentiate enamel from dentine, neither to visualize the dentino-enamel junction, but it revealed the presence of carious region and even the presence of a transitional region between the decayed dentine to the sound one (Figure 2).

A lateral canal could be fine recognized due to water infiltration that occupies its space: it can be differentiate from a microcrack because it's presence is limited to few slices and its signal is brighter than a microcrack that is less hydrated (Figure 4 and 5).

Imaging of all structural components of a tooth with one technique to a single image is still not possible using conventional MRI: constant-time imaging (CTI) combines the advantages of both the standard MRM and the STRAFI and it seemed to be suitable for imaging teeth because it can reproduce both hard and soft tissues. CTI allows the detection of protons in pulp tissue and in hard dental substances so it could clearly differentiate enamel, dentin, and root cementum with a resolution down to 195 μm^3 [27].

In contrast to conventional MRI sequences, Hövener *et al.* (2012) showed that a ZTE acquisition protocol could clearly represents soft tissues as well as solid state components. In addition, the contrast provided by the ZTE sequence allows differentiation between the dental components such as enamel, dentin, cementum and pulp at an isotropic resolution of ~150 μm *ex vivo* [28].

ZTE MRI provided images comparable to MicroCT, which cannot be achieved using conventional MRI or ultrashort echo time imaging UTE. Due to its excellent enamel-dentin contrast given by the increased signal from the dentin, ZTE could be a useful laboratory technique to probe

structural abnormalities such as dental caries even when the tissue appeared normal on visual inspection [29, 30].

The NMR image appearance of decayed dentin is characterized by the enlargement of mineralized tissue porosity which extends the T_2 of spin protons contained in the carious lesion: local acid accumulation due to bacterial inflammation, followed by a demineralization and finally breakdown of the mineral structure and the possible penetration of saliva results in an increased local proton density [31]. The high-intensity signal from water in solution and the lack of signal from mineralized tissues produce contrast that allows recognition of dental crown, outline of the carious lesion, pulp chamber and root canals. Carious tissues provide an intense NMR signal and their image can be readily distinguishable from the other dental tissues: when a three-dimensional reconstruction of the tooth is performed, the extension of the decayed tissues can be easily recognizable. When the decay is extended to the pulp chamber, pulp cavity and the carious tissues can appear as a single structure. It is also possible to determine the presence of a transition zone of increasing demineralization between a very high-intensity area of demineralized tissue and the zero intensity zone of the sound tissue. *In vitro* studies using extracted teeth, acquisition time could vary from minutes to hours: for clinical acquisitions, new devices and techniques were proposed to decrease acquisition time substantially [32, 33].

The clinical applicability of the MRI in diagnosing decays has been demonstrated using the 3D Ultra Short Echo Time sequence (3D UTE MRI) for early identification of demineralization and carious lesions *in vivo*. The application of 3D UTE MRI showed a sensitivity comparable or superior to the common intraoral bitewing x-ray techniques and it may be able to provide a more accurate assessment of the lesion extensions and a better estimation of its distance from the pulp. Despite the high sensitivity provided by this technique, acquisition time and the higher costs still represent a concrete obstacle for a widespread clinical application [33].

The development of volume investigation and MRI microscopy, provided tools for research in endodontics and clinically obtain 3D images of the teeth and root canal systems. MR microscopy has the advantage of obtaining data in a nondestructive way, which could be useful in clinical diagnosis. With a resolution of about 100-300 μm, MRI microscopy could leads to better understand processes that occur inside the teeth during inflammation or in case of narrowing and obstruction of the root canal during repairing processes from secondary and tertiary dentin [34]. Reconstructions from MRI allow to recognize the number of roots, show the anatomy of root canals and the outline of the pulp chamber [35].

When a void is shown by a radiographic or CBCT image, clinicians have no clue whether this area is simply a void due to inadequate root

canal filling procedure or an area filled with left organic debris due to inefficient cleaning and shaping procedures (missed treatment). In this study, MRI was able to distinguish whether a void was filled or not with soft tissue, by determining different water contents and relaxation times. Multi-slice multi echo sequences in this study, showed the presence of an incomplete three-dimensional endodontic gutta-percha filling. Two cones of guttapercha were fine visible and surrounded by water which delineates the apical third shape due to inadequate filling (Figure 7).

In MRI, the pulp chamber of vital teeth is always well represented as structures gave a very clear hyperintense signal. Furthermore, NMR enables optimal assessment of relations between the tooth and a lesion: periodontal space is well defined and NMR demonstrated a high sensitivity for edema and neurovascular bundle. In contrast with CT, dental MRI can give informations about chemical, vascular and edematous properties of a lesion: soft tissue processes like inflammations could be accurately visualized [36].

Enamel and dentin usually appear black due to the lack of unbound protons, on the contrary, the dental pulp chamber which contains nerves, blood vessels and connective tissue, appears white or gray. Surrounding structures were well visualized: cortical bone can be identified as a black zone outlined by moderate signal from external soft tissues.

The root of a non vital tooth, produces a different signal when

compared with a vital one: signal is attenuated or absent due to the presence of necrotic tissues which are no more perfused or by the presence of a root canal obturation. Where vital structures in the root showed a bright MRI signal and could be easily assessed by MRI, the general pulp dehydration with aging and root canal fillings such as gutta-percha, could incapacitate the identification of the root canal and the apical foramen, due to the proper characteristics of such material (gutta-percha cones appear black similar to non-hydrated tissues) [11, 37].

The monitoring of the internal and external root canal morphology is very important for planning a successful endodontic treatment. Many studies attempted to reconstruct the internal and external morphology of human extracted and endodontically treated tooth using MRI. Dragan *et al.* (2016) obtained accurate images of a human endodontically treated wisdom tooth using a 7.04 T device with a True-FISP sequence protocol: the external morphology of mesial and distal roots as well as the correspondingly shaped root canals, root canal curvatures, the furcal region, the interradicular root grooves, and details of the apical finishing of the root canal treatment can be clearly seen in the 3D reconstruction [8].

Newly developed MRI techniques allow imaging of porous solids within minutes: *ex vivo* UTE and ZTE MRI clearly surpass the resolution and information of conventional MRI and CBCT. At an order of

magnitude of ~150 μm isotropic resolution, fine structures like secondary root channels are readily detected and it can be allowed fine segmentation of the pulp. *In vivo* ZTE is still not available and actually it is possible to reach a resolution of ~600 μm within minutes using standard modern equipment and conventional MRI sequences [26].

An *in vivo* study performed by Assaf *et al*. with a 3T NMR scanner for human investigation, testing four different MRI sequences: non contrast-enhanced T_1 weighted (T_1w), non contrast-enhanced fat saturated (fs) T_1w, fst$_2$w and constructive interference steady state (CISS), showed that pulp chamber, periodontal space and eventually periapical lesions were visible even without the use of a contrast media. As expected, differentiation of the enamel-dentin junction and the cementum-dentin junction of the teeth was poor or ineffective [38].

With the aid of dedicated coils, the *in vivo* visibility of the mandibular canal, nutritive canals and periodontal ligaments could be improved: Sedlacik *et al.,* assessed pathological conditions and their relationship to surrounding structures, the pulp chamber and the apical foramen, these informations could lead to a better diagnosis of inflammation and the vitality of the pulp [17].

Idiyatullin *et al.* (2011 and 2016) performed *in vitro* and *in vivo* SWIFT experiments and demonstrated that the dental anatomy could be well resolved, including enamel, dentin and pulp. SWIFT sequence

demonstrated to be able also in detecting microcracks of the tooth *in vitro* and *in vivo* with an acquisition time that could be considered affordable for human investigation (~10 minutes) [16, 39]. MSME sequences used in this study also revealed the presence of microcracks, lesions that are usually invisible to modern CBCT (Figures 5 and 6).

Intrinsic features of the dental MRI could let this method to be capable in the recognition of vital or non-vital teeth: with the use of a contrast media, vital pulp will be brighter, so it could be indicated for older teeth that will result in a lower signal intensity due to the minor perfusion of the pulp; non vital or endodontically treated teeth will not show any brightness. [40, 41]. Dental MRI could also give useful information during the follow up of a tooth transplantation or in case of traumatic dental injuries in children, when the prognosis is doubtful: reperfusion due to revascularization can be shown as a contrast enhancement in the pulp chamber [41, 42].

Necrotic teeth, in case of not performed or unsuccessful endodontic treatment, are commonly affected by chronic periapical periodontitis. In order to be radiographically visible, a periapical radiolucency should reach nearly 30–50% of bone mineral loss. MRI could show periapical lesions in an earlier stage and with smaller bone mineral loss due to its sensitivity to the changes in the T_2 relaxation time of water molecules.

A periapical abnormal area appears gray or white and it can be

distinguished from the bone marrow. When a periapical lesion reached and thinned cortical bone, the last can be visualized as a thin black line narrowing the lesion orally and buccally. Laterally to the lesion, it can be present a black area representing bone sclerosis. NMR can also differentiate the nature of the substances contained in the lesion: the presence of blood or a high protein or high cellular content can be recognizable. Furthermore, MR images could differentiate a simple fluid-filled cavity from an encapsulated cyst: multi-contrast MRI helped with the identification of fluids and fibrous tissues, allowing the identification of the cyst's core and wall or distinguish a radicular cyst from a chronic apical granuloma or other solid odontogenic neoformations. MRI images can also be reconstructed by software which allows measurements to define the volumetric evolution of the lesion over time [17, 38, 44].

Although the radiographic examination remains the method of choice for diagnosis in endodontics, MRI may also take a place in a next future as an adjunct diagnostic device, due to its several advantages. MRI can show not only soft dental and periapical tissues, but also differentiate them, e.g. vessels and nerves, and assess the perfusion and vitality of the tooth: informations that could be very helpful in regenerative techniques, conservative treatments and management of dental trauma injuries [41, 42, 43, 44].

To date, the most powerful magnetic field for dental investigation *in vitro*

was used by Weiger *et al.* (2012): a Bruker BioSpin MRI (GmbH, Ettlingen, Germany) at 11.7 T, demonstrated the ability of the ZTE technique to provide high-resolution and high-quality images of samples with very short T_2. Unfortunately, clinical MRI systems are actually unable to perform the required rapid T/R switching within a couple of microseconds. Furthermore, the large RF amplitudes necessary for generating reasonable flip angles are often not possible with standard RF coils and amplifiers. These limitations are of a technical nature and it could be possible to overcome by the further developments concerning RF devices [27].

5. CONCLUSIONS

The applications of MRI in endodontics might go further than the diagnostic and treatment planning. While hard tissues can be more easily visualized by traditional radiology, MRI is a more suitable technology to visualize the soft pulpar tissues: as opposed to hard dental tissues, soft dental tissues have higher water content and much longer T_2 relaxation times. To date, endodontic procedures have been non-invasively investigated mostly by means of 2D or 3D tooth radiographs, in which soft dental tissues are represented only indirectly as signal voids (empty spaces) inside the tooth.

Based on these concepts and the results of this study, MRI could be used to evaluate the presence of remnants of pulp tissue after endodontic treatment and distinguish these tissues from voids and other specimen *in vitro*. The current standard for the assessment of soft tissues inside the root canals is the histological evaluation, however it is a destructive, time-consuming method that do not allow monitoring of alterations in the same specimen. MRI is currently the only non-invasive technique that enables visualization of soft dental tissues, their differentiation and quantify the amount of soft tissues left inside the endodontic space after the procedures both *in vitro* and *in vivo*.

MRI has the potential to become a more common investigating tool both in research and clinical endodontics. The possibility to evaluate decay

extensions, vitality and vascularization of the pulp, presence of soft tissue remnants after endodontic procedures, early detection and precise follow up periapical lesions, with the great advantage of avoiding the risk of ionizing radiations, should boost up the development of cheaper and compact appliances for everyday clinical use. While some companies are currently developing RF coils located in a narrow area around the teeth, to our knowledge, has not yet developed "localized and tooth dedicated" magnetic field gradient coils for clinical use. However, it can be desirable a widespread use of NMR, similarly to the most common CBCT devices, which are currently used in most dental offices.

Although the radiographic examination will still be the diagnostic method of choice in endodontics, MR imaging may also take its place in future as an adjunct diagnostic tool, due to its several advantages. MRI can visualize soft dental tissues, can differentiate tissues, vessels and nerves in regenerative techniques, and is harmless as it does not involve any ionizing radiation.

In conclusion, is it possible to assess that MRI has a potential to become a valuable, non-invasive device to investigate the endodontic space and consequently assess the quality of cleaning and filling procedures due to its skill in finding and differentiating tissue remnants from endodontic materials, aspects that are usually not detectable with the most common CT, CBCT and Micro-CT devices.

ACKNOWLEDGEMENTS

Prof. Gianluca Gambarini, Department of Oral and Maxillo Facial Sciences, Sapienza University of Rome, Italy for scientific contribution on endodontics.

Prof. Silvia Capuani, CNR ISC Physics Department Sapienza University of Rome, Italy for scientific contribution in physics of Magnetic Resonance and for making available the NMR spectrometer for teeth acquisitions.

Dr. Bruna Mastronicola, Department of Oral and Maxillo Facial Sciences, Sapienza University of Rome, Italy for contribution in literature research.

REFERENCES

1. Baumann MA, Doll GM. Spatial reproduction of the root canal system by magnetic resonance microscopy. J Endod. 1997 Jan;23(1):49-51. PubMed PMID: 9594746.

2. Idiyatullin D, Suddarth S, Corum CA, Adriany G, Garwood M. Continuous SWIFT. J Magn Reson. 2012 Jul;220:26-31. doi: 10.1016/j.jmr.2012.04.016. Epub 2012 May 9. PubMed PMID: 22683578; PubMed Central PMCID: PMC3389185.

3. Olt S, Jakob PM. Contrast-enhanced dental MRI for visualization of the teeth and jaw. Magn Reson Med. 2004 Jul;52(1):174-6. PubMed PMID: 15236382.

4. van Luijk JA. NMR: dental imaging without x-rays? Oral Surg Oral Med Oral Pathol. 1981 Sep;52(3):321-4. PubMed PMID: 6945543.

5. White SC, Pharoah MJ. The evolution and application of dental maxillofacial imaging modalities. Dent Clin North Am. 2008 Oct;52(4):689-705, v. doi:10.1016/j.cden.2008.05.006. PubMed PMID: 18805224.

6. Niraj LK, Patthi B, Singla A, Gupta R, Ali I, Dhama K, Kumar JK, Prasad M. MRI in Dentistry- A Future Towards Radiation Free Imaging - Systematic Review. J Clin Diagn Res. 2016 Oct;10(10):ZE14-ZE19. Epub 2016 Oct 1. Review. PubMed PMID: 27891491; PubMed Central PMCID: PMC5121829.

7. Tymofiyeva O, Proff PC, Rottner K, DUring M, Jakob PM, Richter EJ. Diagnosis of dental abnormalities in children using 3-dimensional magnetic resonance imaging. J Oral Maxillofac Surg. 2013 Jul;71(7):1159-69. doi:10.1016/j.joms.2013.02.014. Epub 2013 Apr 21. PubMed PMID: 23611603

8. Drăgan OC, Fărcăşanu AŞ, Câmpian RS, Turcu RV. Human tooth and root canal morphology reconstruction using magnetic resonance imaging. Clujul Med. 2016;89(1):137-42. doi: 10.15386/cjmed-555. Epub 2016 Jan 15. PubMed PMID: 27004037; PubMed Central PMCID: PMC4777457.

9. Schreiner LJ, Cameron IG, Funduk N, Miljković L, Pintar MM, Kydon DN. Proton NMR spin grouping and exchange in dentin. Biophys J. 1991 Mar;59(3):629-39. PubMed PMID: 2049523; PubMed Central PMCID: PMC1281227.

10. Funduk N, Kydon DW, Schreiner LJ, Peemoeller H, Miljković L, Pintar MM. Composition and relaxation of the proton magnetization of human enamel and its contribution to the tooth NMR image. Magn Reson Med. 1984 Mar;1(1):66-75. PubMed PMID: 6571438.

11. Tutton LM, Goddard PR. MRI of the teeth. Br J Radiol. 2002 Jun;75(894):552-62. PubMed PMID: 12124246.

12. Idiyatullin D, Corum C, Moeller S, Prasad HS, Garwood M, Nixdorf DR. Dental magnetic resonance imaging: making the invisible visible. J Endod. 2011 Jun;37(6):745-52. PubMed PMID: 21787482.

13. Lockhart PB, Kim S, Lund NL. Magnetic resonance imaging of human teeth. J Endod. 1992 May;18(5):237-44. PubMed PMID: 1402579.

14. Lockhart PB, Lund NL, Kim S. Correlation of magnetic resonance image and histology of human teeth. Proc Finn Dent Soc. 1992;88 Suppl 1:161-5. PubMed PMID: 1380714.

15. Sustercic D, Sersa I. Human tooth pulp anatomy visualization by 3D magnetic resonance microscopy. Radiol Oncol. 2012 Mar;46(1):1-7. doi:10.2478/v10019-012-0018-y. Epub 2012 Mar 6. PubMed PMID: 22933973; PubMed Central PMCID: PMC3423768.

16. Idiyatullin D, Corum CA, Nixdorf DR, Garwood M. Intraoral approach for imaging teeth using the transverse B1 field components of an occlusally oriented loop coil. Magn Reson Med. 2014 Jul;72(1):160-5. doi: 10.1002/mrm.24893. Epub 2013 Jul 30. PubMed PMID: 23900995; PubMed Central PMCID: PMC3873378.

17. Sedlacik J, Kutzner D, Khokale A, Schulze D, Fiehler J, Celik T, Gareis D, Smeets R, Friedrich RE, Heiland M, Assaf AT. Optimized 14+1 receive coil array and position system for 3D high-resolution MRI of dental and maxillomandibular structures. Dentomaxillofac Radiol. 2016;45(1):20150177. doi: 10.1259/dmfr.20150177. Epub 2015 Sep 15. PubMed PMID: 26371075; PubMed Central PMCID: PMC5083890.

18. Ludwig U, Eisenbeiss AK, Scheifele C, Nelson K, Bock M, Hennig J, von Elverfeldt D, Herdt O, Flügge T, Hövener JB. Dental MRI using wireless intraoral coils. Sci Rep. 2016 Mar 29;6:23301. doi: 10.1038/srep23301. PubMed PMID: 27021387; PubMed Central PMCID: PMC4810435.

19. Tymofiyeva O, Vaegler S, Rottner K, Boldt J, Hopfgartner AJ, Proff PC, Richter EJ, Jakob PM. Influence of dental materials on dental MRI. Dentomaxillofac Radiol. 2013;42(6):20120271. doi:10.1259/dmfr.20120271. Epub 2013 Apr 22. PubMed PMID: 23610088; PubMed Central PMCID: PMC3667526.

20. Grosse U, Syha R, Papanikolaou D, Martirosian P, Grözinger G, Schabel C, Schick F, Springer F. Magnetic resonance imaging of solid dental restoration materials using 3D UTE sequences: visualization and relaxometry of various compounds. MAGMA. 2013 Dec;26(6):555-64. doi: 10.1007/s10334-013-0373-8. Epub 2013 Mar 23. PubMed PMID: 23525675.

21. Shafiei F, Honda E, Takahashi H, Sasaki T. Artifacts from dental casting alloys in magnetic resonance imaging. J Dent Res. 2003 Aug;82(8):602-6. PubMed PMID: 12885843.

22. Weiger M, Brunner DO, Dietrich BE, Müller CF, Pruessmann KP. ZTE imaging in humans. Magn Reson Med. 2013 Aug;70(2):328-32. doi: 10.1002/mrm.24816. Epub 2013 Jun 14. PubMed PMID: 23776142.

23. Lloyd CH, Scrimgeour SN, Chudek JA, Hunter G, MacKay RL. Application of magnetic resonance microimaging to the study of dental caries. Caries Res. 2000 Jan-Feb;34(1):53-8. PubMed PMID: 10601785.

24. Bracher AK, Hofmann C, Bornstedt A, Hell E, Janke F, Ulrici J, Haller B, Geibel MA, Rasche V. Ultrashort echo time (UTE) MRI for the assessment of caries lesions. Dentomaxillofac Radiol. 2013;42(6):20120321. doi: 10.1259/dmfr.20120321. Epub 2013 Feb 18. PubMed PMID: 23420857; PubMed Central PMCID: PMC3667523.

25. Appel TR, Baumann MA. Solid-state nuclear magnetic resonance microscopy demonstrating human dental anatomy. Oral Surg Oral Med Oral Pathol Oral Radiol Endod. 2002 Aug;94(2):256-61. PubMed PMID: 12221396.

26. Weiger M, Brunner DO, Tabbert M, Pavan M, Schmid T, Pruessmann KP. Exploring the bandwidth limits of ZTE imaging: Spatial response, out-of-band signals, and noise propagation. Magn Reson Med. 2015;Nov;74(5):1236-47. doi: 10.1002/mrm.25509. Epub 2014 Oct 30.

27. Weiger M, Pruessmann KP, Bracher AK, Köhler S, Lehmann V, Wolfram U, Hennel F, Rasche V. High-resolution ZTE imaging of human teeth. NMR Biomed. 2012 Oct;25(10):1144-51. doi: 10.1002/nbm.2783. Epub 2012 Jan 31. PubMed PMID: 22290744.

28. Hövener JB, Zwick S, Leupold J, Eisenbeiβ AK, Scheifele C, Schellenberger F, Hennig J, Elverfeldt DV, Ludwig U. Dental MRI: imaging of soft and solid components without ionizing radiation. J Magn Reson Imaging. 2012 Oct;36(4):841-6. doi: 10.1002/jmri.23712. Epub 2012 Jun 15. PubMed PMID: 22707436.

29. Rychert KM, Zhu G, Kmiec MM, Nemani VK, Williams BB, Flood AB, Swartz HM, Gimi B. Imaging tooth enamel using zero echo time (ZTE) magnetic resonance imaging. Proc SPIE Int Soc Opt Eng. 2015 Mar 19;9417. pii: 94171I. PubMed PMID: 25914509; PubMed Central PMCID: PMC4405678.

30. Bracher AK, Hofmann C, Bornstedt A, Boujraf S, Hell E, Ulrici J, et al. Feasibility of ultra-short echo time (UTE) magnetic resonance imaging for identification of carious lesions. Magn Reson Med 2011; 66: 538–545. PubMed PMID: 21360742.

31. Lloyd CH, Scrimgeour SN, Chudek JA, Hunter G, MacKay RL. Magnetic resonance microimaging of carious teeth. Quintessence Int. 1997 May;28(5):349-55. PubMed PMID: 9452700.

32. Weglarz WP, Tanasiewicz M, Kupka T, Skórka T, Sułek Z, Jasiński A. 3D MR imaging of dental cavities-an in vitro study. Solid State Nucl Magn Reson. 2004 Jan;25(1-3):84-7. PubMed PMID: 14698391.

33. Bracher AK, Hofmann C, Bornstedt A, Hell E, Janke F, Ulrici J, Haller B, Geibel MA, Rasche V. Ultrashort echo time (UTE) MRI for the assessment of caries lesions. Dentomaxillofac Radiol. 2013;42(6):20120321. doi: 10.1259/dmfr.20120321. Epub 2013 Feb 18. PubMed PMID: 23420857; PubMed Central PMCID: PMC3667523.

34. Baumann MA, Schwebel T, Kriete A. Dental anatomy portrayed with microscopic volume investigations. Comput Med Imaging Graph. 1993 May-Jun;17(3):221-8. PubMed PMID: 8402529.

35. Baumann MA, Doll GM, Zick K. Stray-field imaging (STRAFI) of teeth. Oral Surg Oral Med Oral Pathol. 1993 Apr;75(4):517-22. PubMed PMID: 8464619.

36. Nasel C, Gahleitner A, Breitenseher M, Czerny C, Solar P, Imhof H. Dental MR tomography of the mandible. J Comput Assist Tomogr. 1998 May-Jun;22(3):498-502. PubMed PMID: 9606395.

37. Geibel MA, Schreiber ES, Bracher AK, Hell E, Ulrici J, Sailer LK, Ozpeynirci Y, Rasche V. Assessment of apical periodontitis by MRI: a feasibility study. Fortschr Röntgenstr. 2015 Apr;187(4):269-75. doi: 10.1055/s-0034-1385808. Epub 2015 Jan 16. PubMed PMID: 25594373.

38. Assaf AT, Zrnc TA, Remus CC, Schönfeld M, Habermann CR, Riecke B, Friedrich RE, Fiehler J, Heiland M, Sedlacik J. Evaluation of four different optimized magnetic-resonance-imaging sequences for visualization of dental and maxillo-mandibular structures at 3 T. J Craniomaxillofac Surg. 2014 Oct;42(7):1356-63. doi: 10.1016/j.jcms.2014.03.026. Epub 2014 Apr 13. PubMed PMID: 24837485.

39. Idiyatullin D, Garwood M, Gaalaas L, Nixdorf DR. Role of MRI for detecting micro cracks in teeth. Dentomaxillofac Radiol. 2016;45(7):20160150. doi:10.1259/dmfr.20160150. Epub 2016 Jul 25. PubMed PMID: 27402200.

40. Kress B, Buhl Y, Hähnel S, Eggers G, Sartor K, Schmitter M. Age- and tooth-related pulp cavity signal intensity changes in healthy teeth: a comparative magnetic resonance imaging analysis. Oral Surg Oral Med Oral Pathol Oral Radiol Endod. 2007 Jan;103(1):134-7. Epub 2006 Sep 7. PubMed PMID: 17178507.

41. Kress B, Buhl Y, Anders L, Stippich C, Palm F, Bähren W, Sartor K. Quantitative analysis of MRI signal intensity as a tool for evaluating tooth pulp vitality. Dentomaxillofac Radiol. 2004 Jul;33(4):241-4. PubMed PMID: 15533978.

42. Ploder O, Partik B, Rand T, Fock N, Voracek M, Undt G, Baumann A. Reperfusion of autotransplanted teeth--comparison of clinical measurements by means of dental magnetic resonance imaging. Oral Surg Oral Med Oral Pathol Oral Radiol Endod. 2001 Sep;92(3):335-40. PubMed PMID: 11552155.

43. Assaf AT, Zrnc TA, Remus CC, Khokale A, Habermann CR, Schulze D, Fiehler J, Heiland M, Sedlacik J, Friedrich RE. Early detection of pulp necrosis and dental vitality after traumatic dental injuries in children and adolescents by 3-Tesla magnetic resonance imaging. J Craniomaxillofac Surg. 2015 Sep;43(7):1088-93 [doi:10.1016/j.jcms.2015.06.010]. Epub 2015 Jun 17. PubMed PMID: 26165761.

44. Pinto AS, Costa AL, Galvão ND, Ferreira TL, Lopes SL. Value of Magnetic Resonance Imaging for Diagnosis of Dentigerous Cyst. Case Rep Dent. 2016;2016:2806235. Epub 2016 Sep 27. PubMed PMID: 27795861; PubMed Central PMCID: PMC5071551.